Validation of analytical body force model for actuator disc computations

Sørensen, Jens N.; Andersen, Søren J.

Published in:
Journal of Physics: Conference Series

Link to article, DOI:
10.1088/1742-6596/1618/5/052051

Publication date:
2020

Document Version
Publisher's PDF, also known as Version of record

Validation of analytical body force model for actuator disc computations

Validation of analytical body force model for actuator disc computations

Jens N Sørensen and Søren J Andersen

DTU Wind Energy, Technical University of Denmark
Nils Koppels Allé, bldg. 403, 2800 Lyngby, Denmark
Email: jnso@dtu.dk

Abstract. A new analytical model for representing body forces in numerical actuator disc models of wind turbines is compared to results from a BEM model. The model assumes the rotor disc being subject to a constant circulation, modified for tip and root effects. The advantage of the model is that it does not depend on any detailed knowledge concerning the actual wind turbine being analysed, but only requires information of the thrust coefficient and tip speed ratio. The model is validated for different turbines operating under a wide range of operating conditions. The comparisons show generally an excellent agreement with the BEM model, with, however, some deviations of the tangential force in the root area and at small values of the thrust coefficient.

1. Introduction

In numerical computations of wind farms, it is often impossible to resolve the entire rotor blade geometry of the individual wind turbine, and instead the rotor loading is replaced by appropriately determined body forces. The simplest way of implementing body forces is to use the actuator disc concept in the Navier-Stokes equations and to let them be prescribed either as constant loadings or as prescribed radial distributions. For an actual wind turbine, however, this may not comply with the actual shape of geometry and load distributions. In a recent study, Simisiroglou et al. [1] prescribed different axial loadings and found that differences in the shape of the force distribution could be felt in the wake at least five diameters downstream of the turbine. This will affect the inflow conditions to the surrounding turbines in a wind farm. Moreover, as was demonstrated by Porté-Agel et al. [2], it may also be important to include the azimuthal force distribution in the simulations to capture correctly the near-wake behaviour. However, to do this adequately will require full knowledge of the actual geometry, access to airfoil data, and information regarding the operational envelope of the wind turbine. A systematic study on different ways to include body forces has been carried out by van der Laan et al. [3], which showed that knowing the details of the actual loading results in a much more reliable computation of the wake than simply assuming some more or less arbitrary shapes. A problem, however, is that in most cases only crude information is known about the actual turbine, either because geometry and airfoil data are confidential or simply because the developer has not yet decided size and type of the turbines in the initial development phase of a wind farm. There is therefore a need for a method that in a simple way may represent the rotor loading by body forces without prior knowledge of the turbine. Such a model was recently developed and validated on Large Eddy Simulation (LES) actuator disc computations of the Tjæreborg turbine and the DTU 10MW reference rotor; see Sørensen et al. [4]. The validation showed that the model performs excellently under rated wind speeds. The aim of the present

investigation is to validate further the analytical model on different turbines running under different operating regimes, including non-rated conditions.

2. Methodology

The idea behind the analytical model is the assumption that the actuator disc is subject to a constant circulation, corresponding in principle to a Joukowsky rotor, modified with a tip correction, *F(r)*, and a root correction, *g(r)*. Combining this assumption with generic expressions for the axial and tangential loadings, in dimensionless form, the axial and tangential body forces, respectively, read

$$\begin{aligned} \frac{f_z}{\rho U_0^2} &= q_0 \frac{gF}{x}\left(\lambda x + \tfrac{1}{2} q_0 \frac{gF}{x}\right) \\ \frac{f_\theta}{\rho U_0^2} &= \frac{u_D}{U_0} q_0 \frac{gF}{x} \end{aligned} . \tag{1}$$

Here, the body forces are made dimensionless by ρU_0^2, where ρ is the density of air and U_0 is freestream inflow velocity, $x = r/R$ is the dimensionless radial position, $q_0 = \dfrac{\Gamma_0}{4\pi R U_0}$ is the dimensionless circulation, λ is the tip speed ratio, and u_D the velocity acting on the actuator disc. As tip correction we employ the model proposed Glauert [6],

$$F = \frac{2}{\pi}\arccos\left[\exp\left(-\frac{N_b(1-x)}{2\sin\phi}\right)\right], \tag{2}$$

where N_b denotes the number of rotor blades and ϕ is the local flow angle, which approximately can be determined from the formula,

$$\sin\phi = \frac{1}{\sqrt{1+\lambda^2 x^2 / \left(\dfrac{u_D}{U_0}\right)}} . \tag{3}$$

It should be mentioned that we in the original paper [4] used the tip correction of Prandtl. However, to be consistent with usual standards in BEM theory, we employ the tip correction of Glauert. To account for the influence of the hub and the inner non-lifting part of the rotor, a vortex core of size δ is introduced, and an expression for the root correction is proposed as follows,

$$g = 1 - \exp\left[-a\left(\frac{x}{\bar{\delta}}\right)^b\right], \tag{4}$$

where $\bar{\delta} = \dfrac{\delta}{R}$ denotes the dimensionless radial distance to the point where the maximum azimuthal velocity is achieved. With the proposed model, $\bar{\delta}$ typically corresponds to the point where the lifting surface of the rotor starts. In the general case, the relation between the constants *a* and *b* is determined

by differentiating eq. (4) to determine the maximum azimuthal velocity at $x = \overline{\delta}$. Here we assume *g* to be represented by a 4th order polynomial, hence we get the values *b=4* and *a=2.335*.
Integrating the axial load distribution along the blade and introducing the thrust coefficient $C_T = \dfrac{T}{½\rho\pi R^2 U_0^2}$, the dimensionless reference circulation is determined as,

$$q_0 = \frac{\sqrt{16\lambda^2 a_2^2 + 8a_1 C_T} - 4\lambda a_2}{4a_1}. \tag{5}$$

with the coefficients determined as

$$a_1 = \int_0^1 \frac{g^2 F^2}{x} dx \quad \text{and} \quad a_2 = \int_0^1 gFx dx. \tag{6}$$

The moment acting on the rotor is given by integration of the azimuthal force,

$$M = \int_{AD} r f_\theta dA = 2\pi R^3 \int_0^1 x^2 f_\theta dx. \tag{7}$$

Assuming here a constant inflow, the resulting power coefficient is given as

$$C_P = \frac{M\Omega}{½\rho\pi R^2 U_0^3} = 4\lambda q_0 a_2 \left(\frac{u_D}{U_0}\right), \tag{8}$$

from which the inflow velocity is determined as

$$\left(\frac{u_D}{U_0}\right) = \frac{C_P}{4\lambda q_0 a_2}. \tag{9}$$

Since λ is an input variable and the circulation essentially is a function of tip speed ratio and thrust coefficient, $q_0 = q_0(\lambda, C_T)$, the dimensionless body forces are uniquely determined from λ, C_T and C_P. For more details about the analytical model, we refer the reader to the article by Sørensen et al. [4].

3. Results

In the following we show some significant comparative results for a range of wind turbines operating at different conditions. The BEM computations are carried out using full knowledge regarding the actual blade geometry and associated airfoil data. The operational conditions contain all kinds of combinations between the tip speed ratio and the thrust coefficient, including high wind speeds, corresponding to low thrust coefficients. In this case, the thrust coefficient is lowered by pitching the rotor blades. In contrast to this, the analytic model only demands tip speed ratio, and thrust and power coefficients as input. The computations are carried out for a constant axial inflow without shear and turbulence. As demonstrated in [4], shear and turbulence are easily introduced into the model when carrying out actual CFD/actuator disc computations, and it is not the objective of the present work to include this. Here we focus on

assessing the models ability to represent loadings for different turbines operating both at design and off-design conditions. The chosen wind turbines represent sizes with a range of nameplate capacity from 225 kW to 10 MW. The data for the wind turbines are given below in Table 1, which shows name plate capacity, rotor diameter and design tip speed ratio The latter information is included to assess where we expect the best agreement between the analytical model and the BEM computations.

Table 1. Wind turbine characteristics

	Vestas V27	Vestas V52	NEG Micon NM80	DTU 10MW reference turbine
Name plate capacity [kW]	225	850	2,750	10,000
Diameter [m]	27	52	80	178
Design tip speed ratio [-]	7.6	8.3	8.6	7.5

In the following we compare dimensionless normal and tangential load distributions along a blade. The distributions are normalized by $\rho R U_0^2$, hence the dimensionless quantities are given as,

$$C_n = \frac{F_n\ [N/m]}{\rho R U_0^2}; \qquad C_t = \frac{F_t\ [N/m]}{\rho R U_0^2}\ , \tag{10}$$

where F_n is the normal loading and F_t is the tangential loading on each blade. As the analytical loads in eq. (1) are given per area unit for the full rotor, the load coefficients are computed as

$$C_n = \left(\frac{f_z}{\rho R U_0^2}\right)\cdot\left(\frac{2\pi x}{N_b}\right); \qquad C_t = \left(\frac{f_\theta}{\rho R U_0^2}\right)\cdot\left(\frac{2\pi x}{N_b}\right), \tag{11}$$

where N_b denotes the number of blades.

In Figs. (1) – (8) the load distributions are compared for the different wind turbines operating at various conditions. On each plot, only one of the curves is close to the design conditions, whereas the rest are for off-design conditions, where the turbine is either pitch-regulated or running at upstart conditions. The only input to the analytical model are the tip speed ratio, and the C_T and C_P values from the BEM computations. Figs. (1) and (2) show the load distributions for the V27 rotor (see details in [7] and [8]) . It is here seen that the analytical model represent the normal force distribution quite well. There are some minor differences near the tip, but otherwise the agreement is excellent for all operating conditions. For the tangential force distribution the agreement is excellent near design conditions However, it is also clear that the agreement is less convincing at small thrust coefficients, where the BEM computations show a decreasing tangential force distribution along the blade that is not fully captured by the analytical distribution. This is to be anticipated, however, as the flow in the inner part of the blade starts to stall at high wind speeds. Although the pitch regulation ensures small angles of attack at the outer part of the blade, high wind conditions involves high angles of attack at the inner part of the blade. The same tendencies as those for the V27 turbine are seen for the V52 turbine [9] in Figs. (3) and (4), where the agreement, however, is less convincing for the normal force distribution and slightly better for the tangential loading. It is furthermore seen that a good agreement between BEM results and the analytical model exists for thrust coefficients down to 0.3. Only at as low values as 0.2,

the distributions exhibit different behaviour, where the distribution of the tangential loading attains a distinct maximum at the inner part of the blade (see Fig. 4). From Figs. (5) and (6) it is seen that the analytical load distributions of the NM80 turbine [10] are in very good agreement with the BEM results. Particularly those closest to the design values are in excellent agreement with BEM values. The same tendency is seen for the DTU 10 MW reference rotor [11] in Figs. 7 and 8, where the tangential load distribution first start to differ at a thrust coefficient less than 0.2.

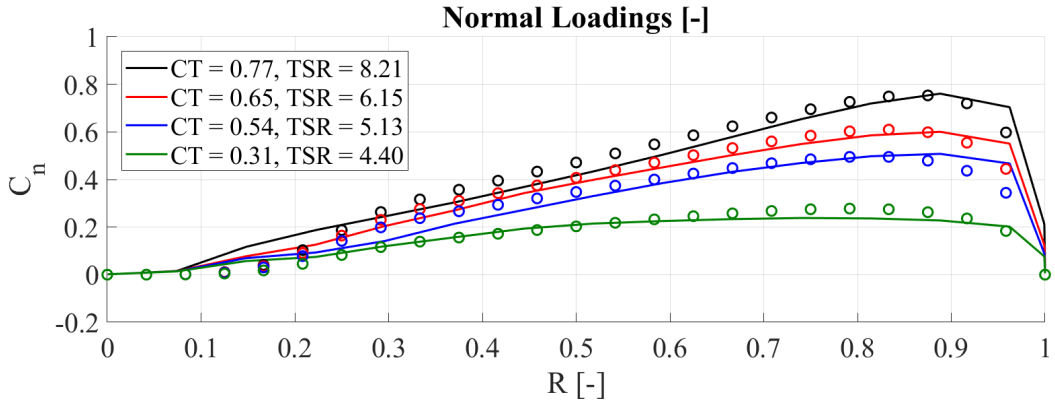

Fig. 1. Normal force coefficient distribution of the V27 turbine at different tip speed ratio and thrust coefficient. Circles: Analytical model; Solid lines: BEM computations.

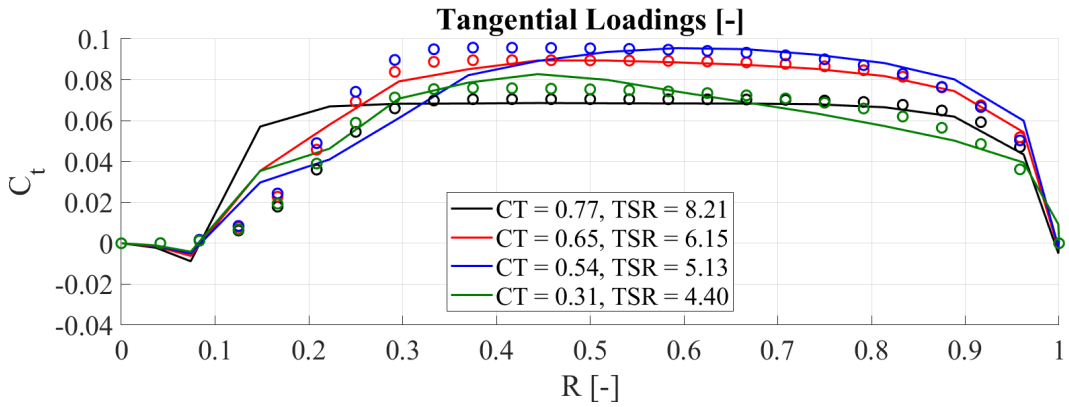

Fig. 2. Tangential force coefficient distribution of the V27 turbine at different tip speed ratio and thrust coefficient. Circles: Analytical model; Solid lines: BEM computations.

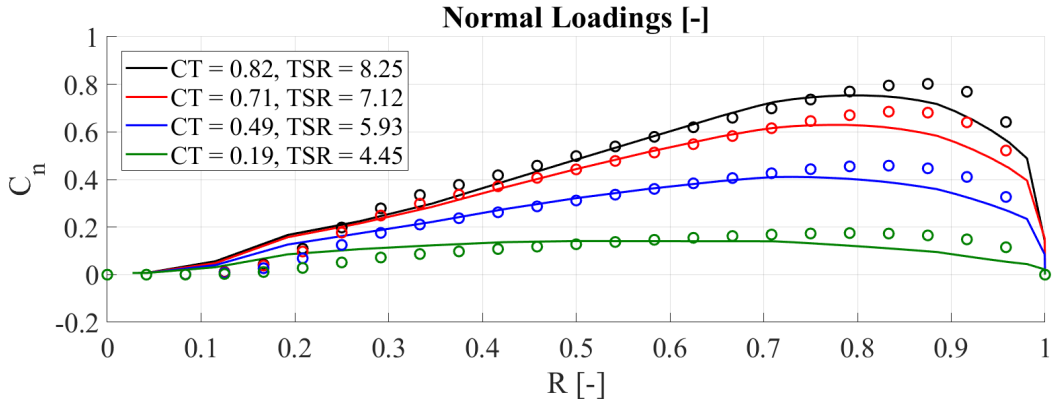

Fig. 3. Normal force coefficient distribution of the V52 turbine at different tip speed ratio and thrust coefficient. Circles: Analytical model; Solid lines: BEM computations.

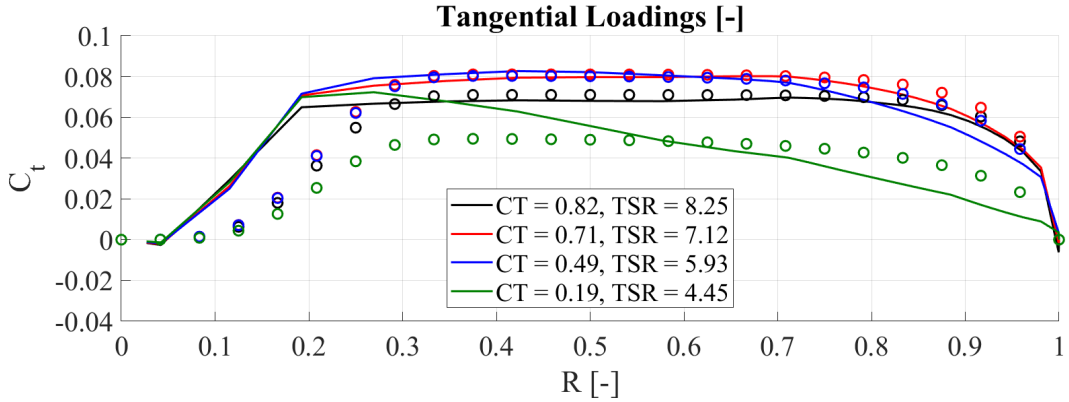

Fig. 4. Tangential force coefficient distribution of the V52 turbine at different tip speed ratio and thrust coefficient. Circles: Analytical model; Solid lines: BEM computations.

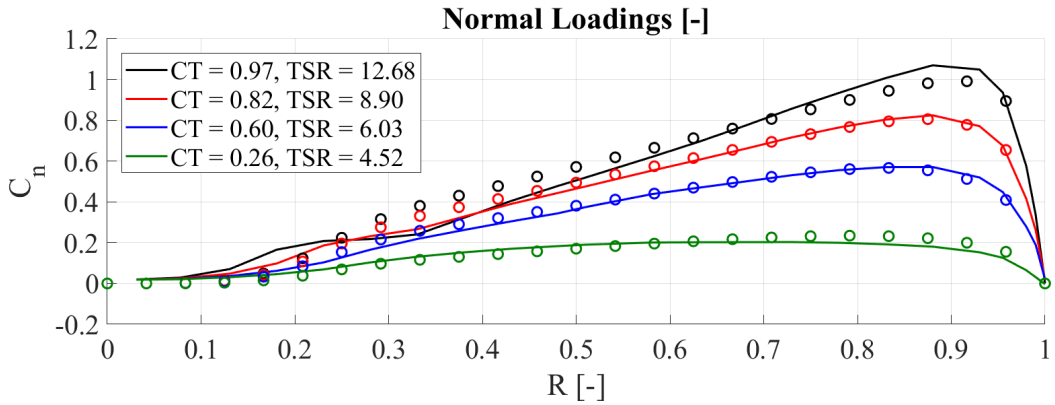

Fig. 5. Normal force coefficient distribution of the NM80 turbine at different tip speed ratio and thrust coefficient. Circles: Analytical model; Solid lines: BEM computations.

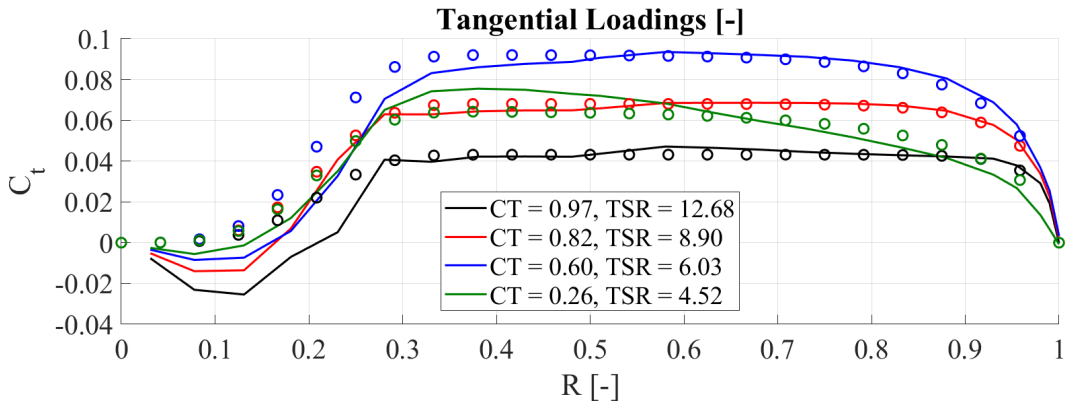

Fig. 6. Tangential force coefficient distribution of the NM80 turbine at different tip speed ratio and thrust coefficient. Circles: Analytical model; Solid lines: BEM computations.

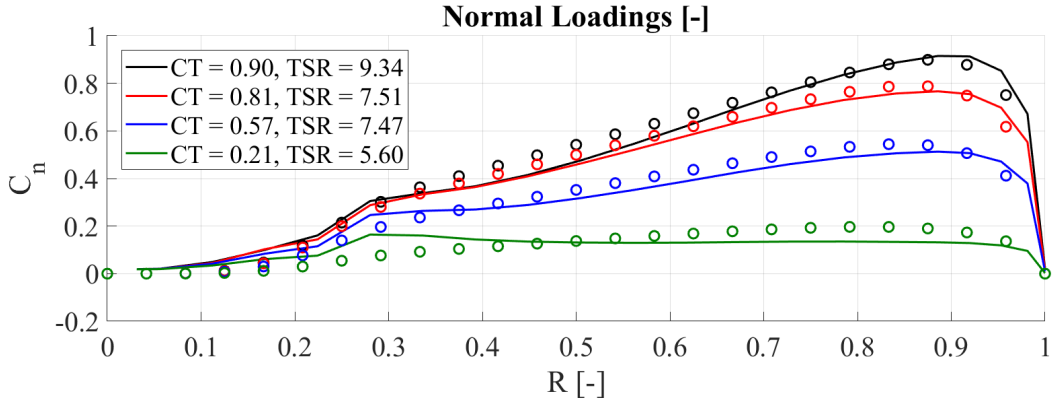

Fig. 7. Normal force coefficient distribution of the DTU 10MW turbine at different tip speed ratio and thrust coefficient. Circles: Analytical model; Solid lines: BEM computations.

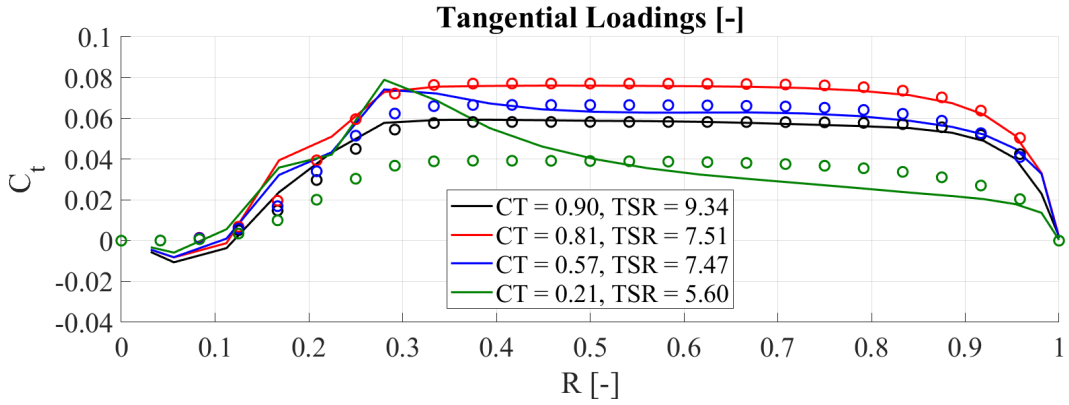

Fig. 8. Tangential force coefficient distribution of the DTU 10MW turbine at different tip speed ratio and thrust coefficient. Circles: Analytical model; Solid lines: BEM computations.

4. Conclusions

An analytical body force model has been validated against load distributions generated by a BEM model. The comparisons were carried out using four turbines of different sizes and operational conditions. The results are very convincing, showing generally a very good agreement between the simple analytical model and the BEM results. The comparison shows that the simple analytical model with good precision can be utilized to represent the loading on wind turbines, both at design and off-design conditions. The characteristics of the tangential loading derived by the analytical model only starts to deviate from the one computed using the BEM model for thrust coefficients lower than 0.3. The deviations occur in the root region as impact of flow separation that is not accounted for with the proposed method. However, this is at an operational condition where the exact knowledge of the tangential load is not important for computing e.g. the overall performance of a wind farm. Hence, we may conclude that the analytical model with good accuracy can be used to represent the loading of most turbines operating both at design and off-design conditions.

5. References

[1] N. Simisiroglou, S. Sarmast, S.-P. Breton, S. Ivanell (2016) Validation of the actuator disc approach in PHOENICS using small scale model wind turbines. J. Physics: Conference Series **753**, 032028. IOP Publishing.Doi:10.1088/1742-6596/753/3/032028.

[2] F. Porté-Agel, Y.T. Wu, H. Lu, R. Conzemius (2011) Large-eddy simulation of atmospheric boundary layer flow through wind turbines and wind farms. J. Wind Eng. Ind. Aerodyn. 99, 154–168.

[3] P. van der Laan, N.N. Sørensen, P.-E. Réthoré, J. Mann, M.C. Kelly, N. Troldborg (2015) The $k-\varepsilon-f_p$ model applied to double wind turbine wakes using different actuator disk force methods. Wind Energy vol. 18(12), 2065-2084.

[4] Sørensen, J.N., Nilsson, K., Ivanell, S., Asmuth, H., Mikkelsen, R.F. (2019) Analytical body forces in numerical actuator disc model of wind turbines. Renewable Energy, vol. 147, 2259-2271.

[5] Øye, S. (996) FLEX4 simulation of wind turbine dynamics. In: Proceedings of the 28th IEA Meeting of Experts Concerning State of the Art of Aeroelastic Codes for Wind Turbine Calculations (Available through International Energy Agency).

[6] Glauert, H. (1935) Airplane Propellers. Division L in *Aerodynamic Theory*, vol. IV, Durand WF (ed.). Springer: Berlin, pp. 169–360.

[7] Resor, B. H., LeBlanc, B., (2014), An Aeroelastic Reference Model for the SWIFT Turbines. SAND2014-19136.

[8] Kelley, C. L., White, J. (2018) An Update to the SwiFT V27 Reference Model. SAND2018-11893

[9] https://en.wind-turbine-models.com/turbines/71-vestas-v52 .

[10] Troldborg, N., Bak, C., Aagaard Madsen, H., Skrzypinski, W. R. (2018) DANAERO MW: Final Report. DTU Wind Energy. DTU Wind Energy E, No. 0027(EN).

[11] Bak, C., Zahle, F., Bitsche, R., Kim, T., Yde, A., Henriksen, L. C. Natarajan, A., Hansen, M. H. (2013) Description of the DTU 10 MW Reference Wind Turbine, DTU Wind Energy Report-I-0092.